

Sea of Galilee: Comprehensive analysis of magnetic anomalies

Lev Eppelbaum,^a Zvi Ben-Avraham,^a Youri Katz,^b and Shmuel Marco^b

^aDepartment of Geophysics and Planetary Sciences, Raymond and Beverly Sackler Faculty of Exact Sciences,
Tel Aviv University, Tel Aviv 69978, Israel

^bPaleontological Division of Zoological Museum, Department of Zoology, Faculty of Life Sciences, Tel Aviv University,
Tel Aviv 69978, Israel

(Received 20 October 2003; accepted in revised form 19 September 2004)

Abstract

Eppelbaum, L., Ben-Avraham, Z., Katz, Y., and Marco, S. 2004. Sea of Galilee: Comprehensive analysis of magnetic anomalies. *Isr. J. Earth Sci.* 53: 151–171.

A variety of magnetic sources occurring in the Sea of Galilee (Lake Kinneret) and around the lake cause a complex pattern of anomalous magnetic field. Positive and negative magnetic anomalies in the Kinneret basin correspond to basalts of normal and reverse magnetization, respectively. Using interpretation methods specially developed for complicated geological conditions (improved versions of characteristic point, tangent, and areal methods), we determined the quantitative parameters of the anomalous bodies and performed their classification. We applied 3-D magnetic field modeling techniques for confirming the data obtained during the quantitative interpretation stage and the effects computing from geological structures. We showed that the paleomagnetic zones identified in the lake basin are in accordance with the western and northern margins of Lake Kinneret, but are incongruent with the eastern and southern margins. Based on radiometric and paleomagnetic data analysis, we can conclude that Early Pliocene basaltic flows cover the western part of Lake Kinneret. A N–S paleomagnetic profile suggests that the western part of the Lake Kinneret depression may be interpreted as an inversion trough formed in the area of Pliocene uplift in the eastern part of the Galilee. We applied combined geophysical, structural, and tectonic analysis to compile a structural map of the Cover Basalt for Lake Kinneret and adjacent areas.

INTRODUCTION

The Sea of Galilee (Lake Kinneret) is situated in one of the morphotectonic depressions that are located along the Dead Sea Transform (DST) (Fig. 1). This transform is more than 1000 km long, and is a plate boundary separating the Sinai and Arabia plates (Garfunkel et al., 1981). The structure of the Kinneret basin appears to be complex because two fault systems

intersect in the lake's area (Freund, 1970; Rotstein et al., 1992; Ben-Avraham et al., 1996; Heimann et al., 1996; Belitzky, 2002; Hurwitz et al., 2002; Matmon et al., 2003).

Geological studies indicate that rock outcrops in this area and rock samples from wells range from Jurassic to Quaternary. The present configuration of

E-mail: lev@frodo.tau.ac.il

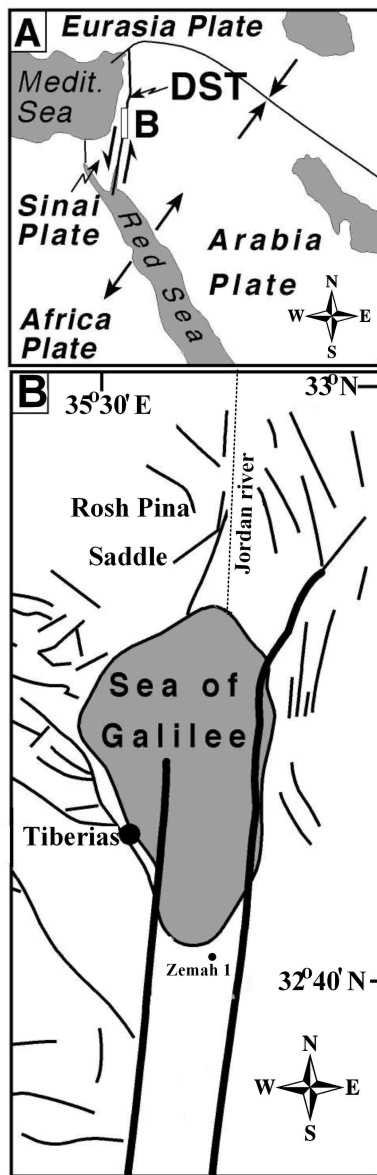


Fig. 1. (A) Regional tectonic setting of the Eastern Mediterranean. (B) The area of study (after Bartov, 1979, Ben-Avraham et al., 1990, and Marco et al., 2003).

the Sea of Galilee was formed about 24,000 years ago (Hazan et al., 2002).

Previous geophysical studies of Lake Kinneret included seismic refraction and reflection measurements using various methods (Ben-Avraham et al., 1981, 1986; Hurwitz et al., 2002), magnetic measurements (Folkman and Yuval, 1976; Ben-Avraham et al., 1980; Ginzburg and Ben-Avraham, 1986), heat flow measurements (Ben-Avraham et al., 1978), gravity mea-

surements (Ben-Avraham et al., 1996), and electromagnetic field analysis (Goldman et al., 1996). Ben-Avraham et al. (1990) mapped the bathymetry of the lake in great detail. A few seismic profiles were obtained north and south of the lake (Rotstein and Bartov, 1989; Rotstein et al., 1992). In this paper, the results of a study of the magnetic field over the lake and their implication to the basalt distribution in this area are presented and discussed. In an ancillary study, Eppelbaum et al. (2004) developed chronostratigraphical and magnetostratigraphical scales of Late Cenozoic basaltic formations in the Lake Kinneret area and presented a scheme of paleomagnetic, magnetic, and radiometrical characteristics of basalt formations in the Lake Kinneret area.

GEOLOGICAL SETTING

Cenozoic volcanism in northern Israel makes up a part of a larger volcanic field extending from the eastern Galilee to western and southern Syria, through Jordan, to Saudi Arabia (Garfunkel, 1989; Heimann et al., 1996; Ilani et al., 2001). The basaltic formation occurrences around Lake Kinneret make up the western part of the northern continuation of the Harrat e-Shamah volcanic field, covering a total area of about 40,000 km² (Weinstein et al., 1994). Eruptions in northern Israel started in the Miocene and continued in several phases until recent times (Freund et al., 1970; Nur and Helsey, 1971; Mor, 1986; Heimann, 1990; Shaliv, 1991; Ilani et al., 2001).

Two series of basalts—Early Cretaceous and Late Cenozoic—are present in the upper part of the geological section. In the vicinity nearest Lake Kinneret the thickness of the Early Cretaceous basalts is minimal (Katz and Eppelbaum, 1999), and hence their contribution to the total magnetic field is negligible. The Late Cenozoic basalts range from Miocene to Pleistocene. They are divided into Lower Basalt (Early–Middle Miocene), Intermediate Basalt (Late Miocene), Cover Basalt (Early Pleistocene), Yarmouk Basalts (Middle Pleistocene), Post-Cover and Ruman Basalts (Late Pleistocene), and Raqqad Basalts (Late Pleistocene) (Heimann, 1990; Shaliv, 1991). The majority of the surface outcrops of basalts surrounding the lake are of Pliocene and Pleistocene age (Heimann et al., 1996; Flexer et al., 2000).

Several fault systems exist in this area, the main ones being the N–S transform system, and the E–W and NW–SE fault systems that break up the eastern Galilee (Golani, 1962; Saltsman, 1964; Schulman,

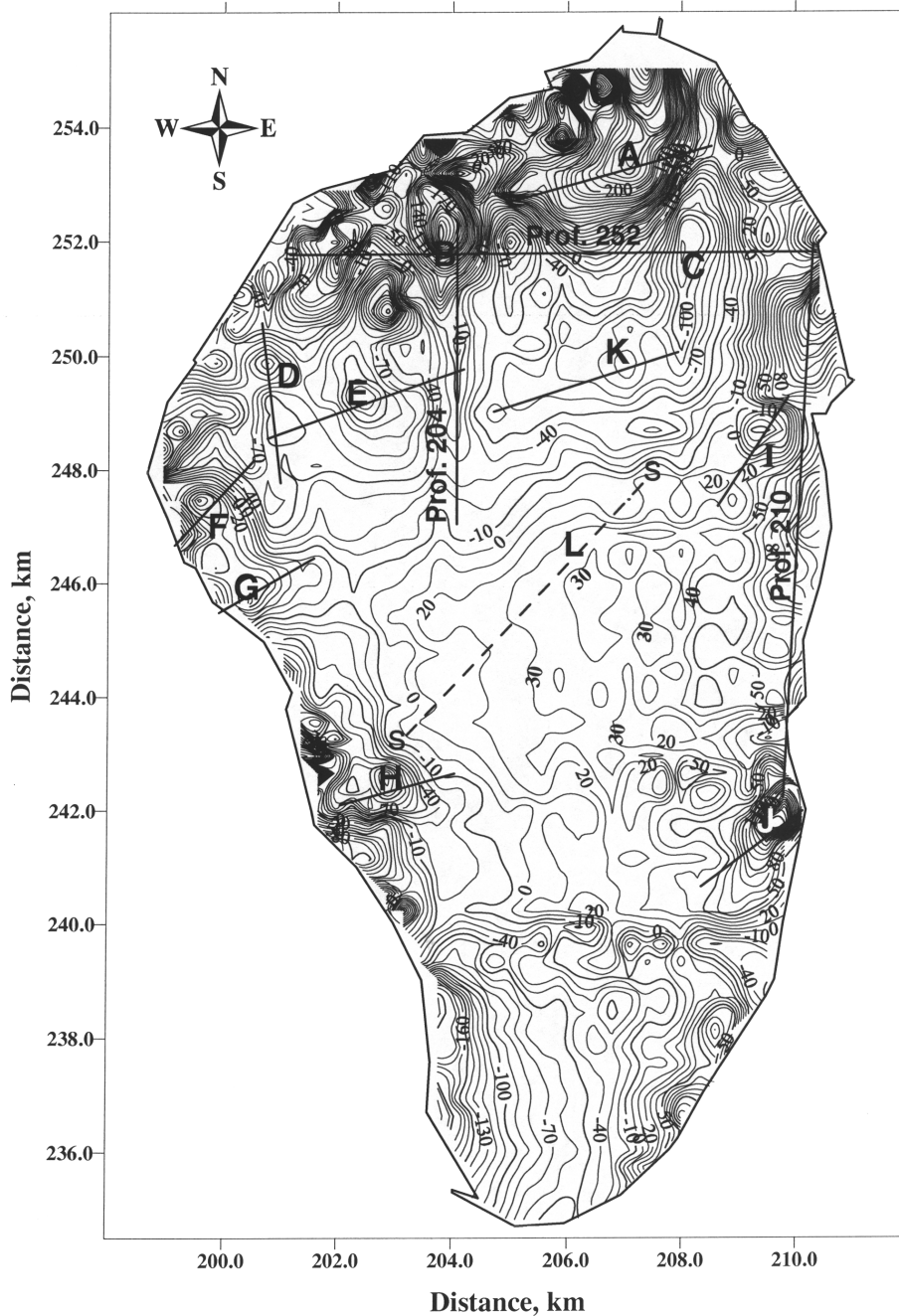


Fig. 2. Map of the total magnetic field (ΔT) of Lake Kinneret with location of the analyzed anomalies and interpretation profiles (data from Ben-Avraham et al., 1980). Isolines are given in nanoTesla.

1966) and the Golan east of the Kinneret (Michelson, 1972). Lake Kinneret and the plain south of it are located in a depression bounded on the east and west by active fault scarps with steep gradients (Garfunkel et al., 1981).

The results of seismic surveys (Ben-Avraham et al., 1986; Hurwitz et al., 2002; Zurieli, 2002) show evidence of active faulting. High heatflow averaged value (93.4 mW/m^2) measured in Lake Kinneret (Ben-Avraham et al., 1978) and earthquake-induced surface

ruptures observed in the vicinity of the lake (Marco et al., 1997, 2003) also indicate tectonic activity.

Superposition of vertical displacements perpendicular or oblique to the transform created complex structures in this area. Since Pliocene and Pleistocene basalt flows and intrusions of variable thickness cover the area (Saltsman, 1964; Schulman, 1966; Neev, 1978; Mor, 1986; Sneh et al., 1998b), structural interpretation of the Kinneret basin by conventional methods is complicated.

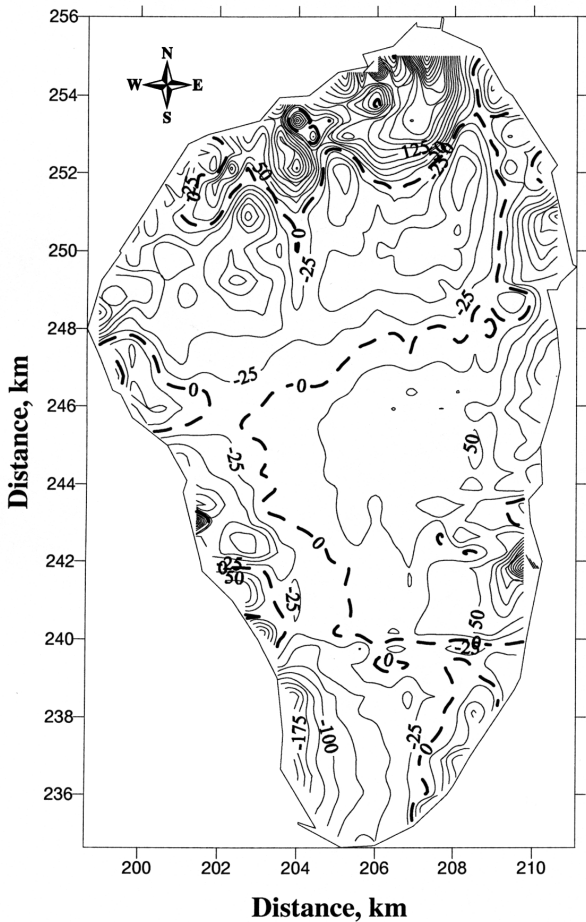
ANALYSIS OF MAGNETIC DATA

Initial magnetic data processing

The first magnetic map of the Lake Kinneret area with a 50 nT isoline interval was constructed by Ben-

Avraham et al. (1980). The authors concluded that considerable anomalies near the margins of the lake may have been caused by fault-controlled occurrences of volcanic rocks, while the central portion of the lake is magnetically quiet. The computed version of the map (Fig. 2) is similar in general to the hand-contoured versions (Ben-Avraham et al., 1980; Ginzburg and Ben-Avraham, 1986), but it allows performing detailed interpretation of magnetic anomalies. The magnetic survey conducted by Ben-Avraham et al. (1980) is characterized by the following characteristics: total number of values—3081; maximum value—614.6 nT; minimum value—(-283.5) nT; mean value—(-0.08) nT; and standard Pearson deviation—81.16 nT. Analysis of the magnetic map shows a very complex magnetic field distribution pattern. This

A Map of vertical gradients of magnetic field



B Map of horizontal gradients of magnetic field

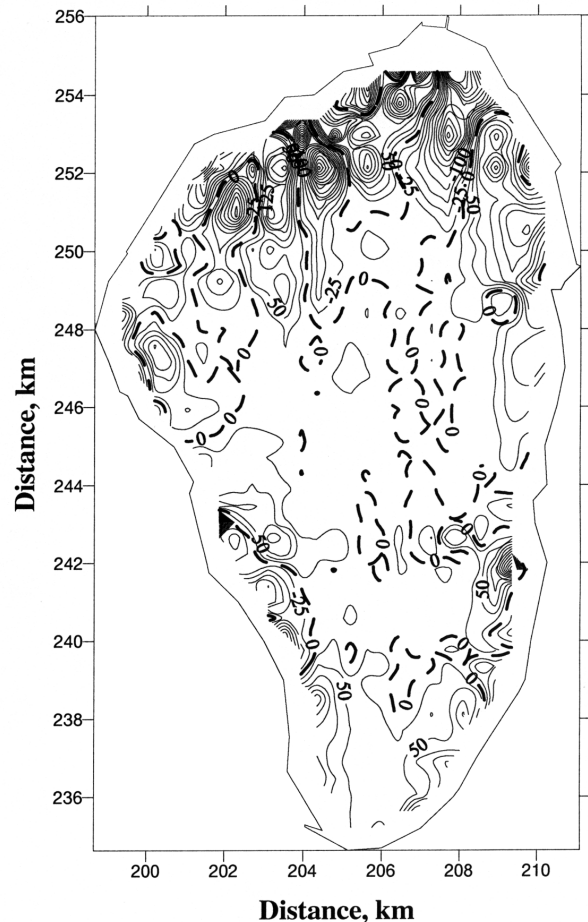


Fig. 3. Maps of the ΔT gradients: (A) vertical gradients, (B) horizontal gradients.

figure continues next page

complex pattern is caused by the combined effect of basalts surrounding the lake and magnetic sources present in the lake.

The vertical and horizontal gradient maps of the ΔT (total magnetic field) (Figs. 3A and 3B, respectively) show the mosaic character of the magnetic field distribution. Anomalous values of the magnetic gradients are displayed, mainly within the lake's borderlines. In both the vertical and the horizontal derivative maps, a complex pattern of the fields in the northern part of Lake Kinneret can be recognized, caused by a variety of different anomalous objects. At the same time, only the vertical gradient map indicates significant field decrease in the E–W direction in the southern part of Lake Kinneret. The computed map of the total magnetic gradient is more smoothed (Fig. 3C), but basi-

cally coincides with the maps of the horizontal and vertical gradients.

Quantitative interpretation of magnetic anomalies

Some principles of magnetic data analysis under oblique magnetization

The major principles of quantitative interpretation, formalized for vertical magnetization, do not work in conditions of oblique magnetization, in low and central latitudes. The inclination of the total magnetic field in Israel ranges from 46° in the north to 42° to the south. Such conditions strongly complicate the interpretation of magnetic data using conventional procedures.

It should be noted that ΔT anomaly distortions occur not only due to the inclination of the magnetization vector to the horizon plane, but also due to the different orientation of the horizontal magnetization projection with respect to the body's axes (Parasnis, 1997). Besides the geomagnetic field inclination, the orientation of the body's axes relative to the horizontal component of the geomagnetic field is also significant. Therefore, the analysis of field graphs is not sufficient; it is necessary to analyze field isoline maps as well (Khesin et al., 1996).

In conditions of oblique magnetization, the "reduction to pole" procedure is often used—calculation of pseudogravitometric anomalies (Blakely, 1995). However, the procedure is suitable only when all interfering bodies in the studied area are magnetized parallel to the geomagnetic field and simultaneously when the bodies have subvertical dipping. Only in this case can the magnetic fields be recalculated correctly; the obtained graphs would be symmetrical, and further interpretation using conventional methods can be done. Similar approaches based on the transformation of the observed magnetic field (for instance, analytic signal (Roest et al., 1992)) have the same limitations.

Our interpretation involves the application of methods developed especially for quantitative interpretation of magnetic anomalies in complex environments (Khesin et al., 1996). Unlike some conventional techniques (Rao and Babu, 1984; Thurston and Smith, 1997; Telford et al., 1999), these methods are applicable in conditions of oblique magnetization, rugged relief, and unknown level of the normal field.

We employed improved modifications of the *characteristic point method*, the *tangent method*, and the *areal method*, utilizing the most commonly applied geometric models such as thin bed, horizontal circular cylinder, and thick bed (Fig. 4). These three geometric

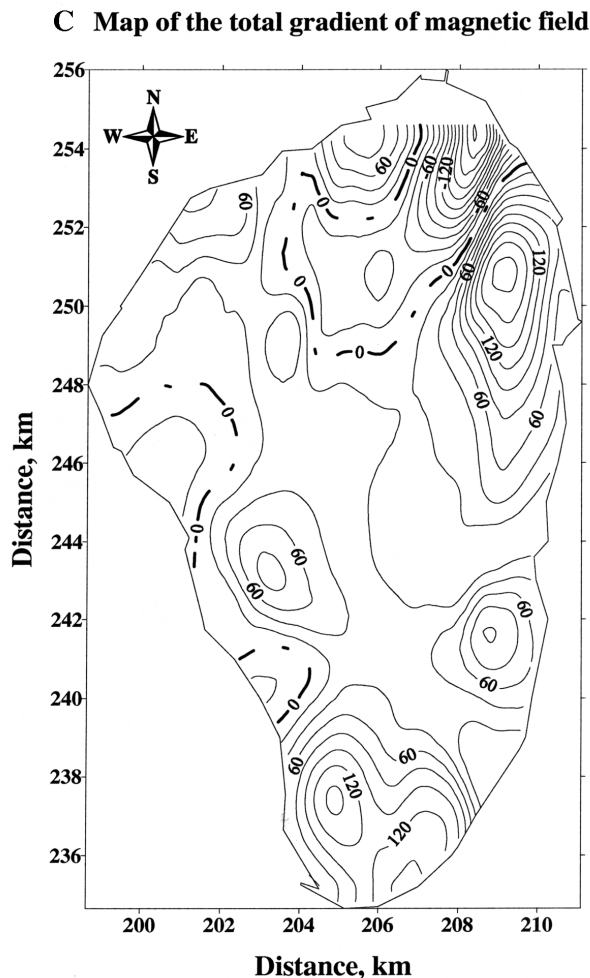


Fig. 3 continued. (C) smoothed total gradient. Isolines are given in nanoTesla.

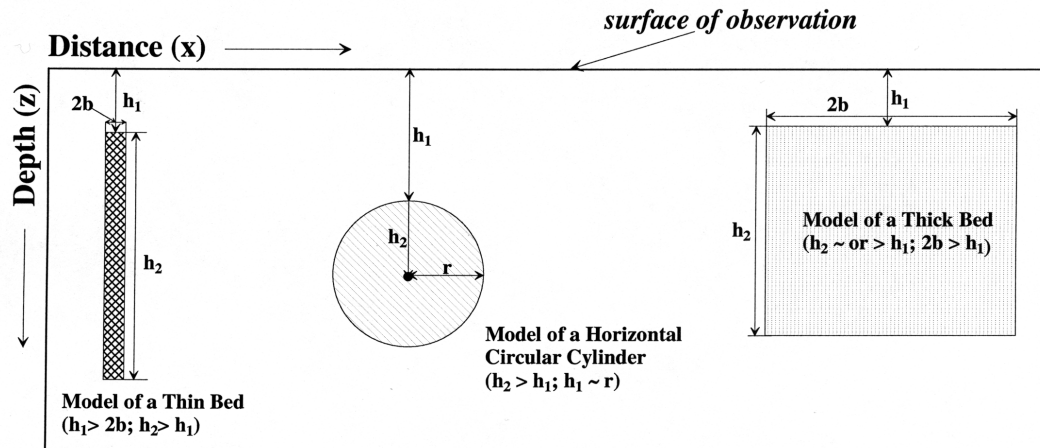


Fig. 4. Models of anomalous bodies based on quantitative interpretation of magnetic anomalies.

models, with different modifications, may be used for approximation and corresponding quantitative interpretation of anomalies generated by various geological objects.

The following parameters are taken from the anomaly plot in the *characteristic point method*: d_1 = difference of semiamplitude point abscissae, d_2 = difference of extremum abscissae, d_3 = difference of inflection point abscissae.

In the *tangent method* four tangents are employed: two horizontal lines with respect to the anomaly extrema and two inclined lines passing through the points of the bend on the left- and right-hand branches of the anomaly plot. The following terms are taken from the plot: d_3 = difference in abscissae of the points of intersection of an inclined tangent with horizontal tangents on one branch; d_4 = the same on the other branch (d_3 is selected from the plot branch with conjugated extremums).

The *areal method* is based on calculation of separate areas limited by the anomalous curve, a horizontal line, and two vertical lines crossing some singular points at the anomalous curve.

A detailed description of the above-mentioned methods is given in Khesin et al. (1996). Magnetic field computing was performed using a specially developed GSFC program (Geological Space Field Calculation) (Eppelbaum et al., 1992; Khesin et al., 1996).

Quantitative interpretation of the Zemah anomaly

The methods developed for advanced magnetic data interpretation (Khesin et al., 1996) were tested on the Zemah magnetic anomaly. The “Zemah 1” well

was drilled about 2 km south of Lake Kinneret. A K/Ar mineral age for a sample from the basalt flow at a depth of 679 m was determined as about of 4.4 Ma (Marcus and Slager, 1985; Heimann et al., 1996), which corresponds to Pliocene. The estimated magnetic effect of the gabbro interbedding is not significant. The results of the quantitative interpretation (upper edge of magnetic body determined at 515 m) are in agreement with the drilling data (489 m) (Figs. 5A,B). The interpretation error is about 5%, which is a good result for such complex environments.

Analysis of selected anomalies

Both positive and negative magnetic anomalies have been identified in the Lake Kinneret basin. We suggest that reversely magnetized basalts cause the negative magnetic anomalies. Two approximation models—thin bed (TB) and horizontal circular cylinder (HCC)—were used (Figs. 6–8). Comprehensive analysis of anomaly A (Fig. 6) indicates that this anomaly is caused by the integrated effect of a few different magnetic sources occurring at different depths, the largest of which is an isometric body (approximated as HCC). The calculated depth to the center of the HCC is 1300 m, and its upper edge is at a depth of 1050–1100 m. Presence of the geological objects approximated by the HCC model may be explained by the presence of separate tectonic blocks occurring at different depths. Anomaly B (for which the TB model was used) was interpreted twice: in the W–E and S–N directions (Fig. 7), with similar results (the depth for the upper edge of the disturbing body is 450 m for the latitudinal profile and 440 m for the

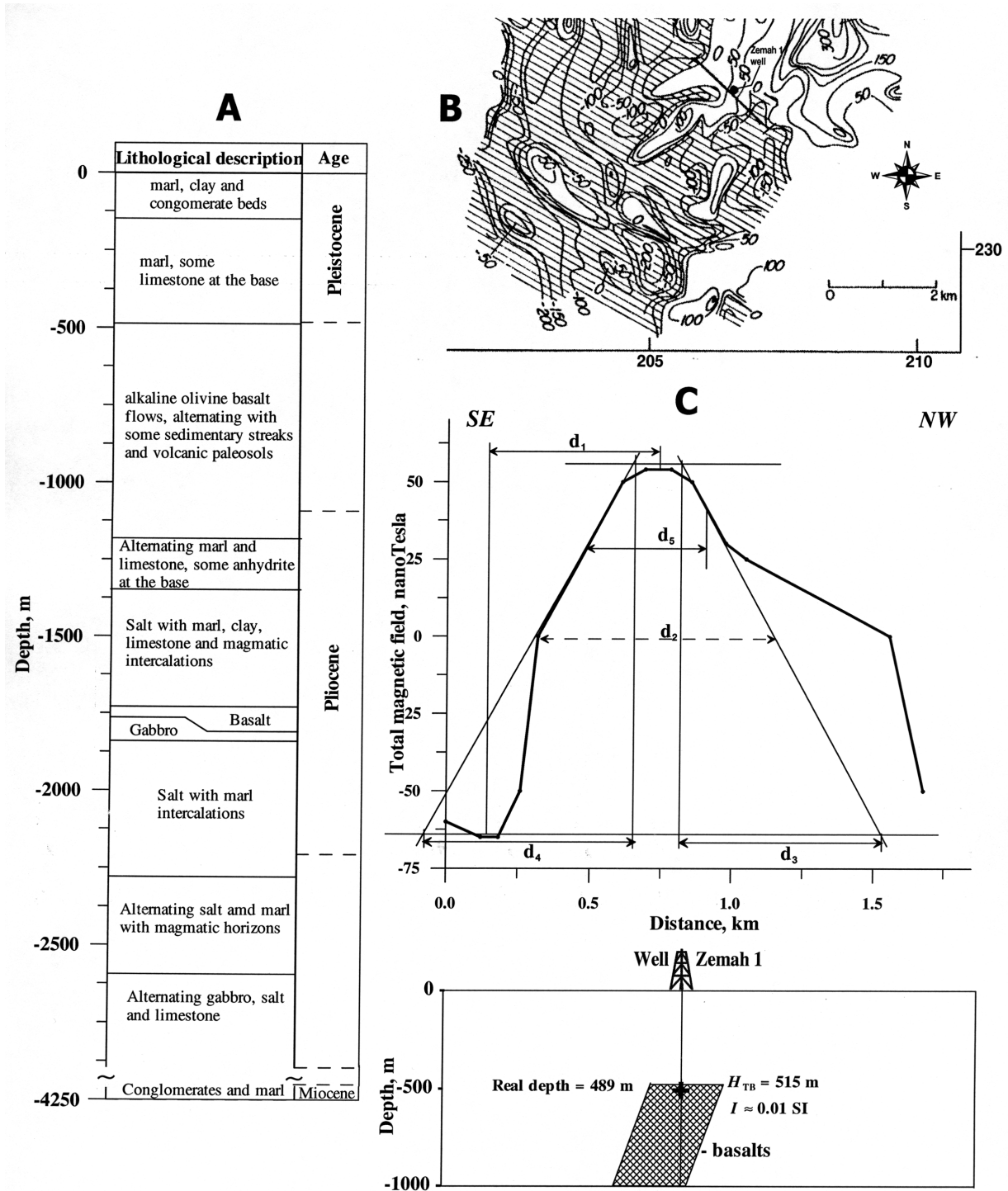


Fig. 5. (A) Simplified lithological description of the Zema 1 well (after Marcus and Slager, 1985); (B) Map of the total magnetic field of Zema area and location of interpreting profile (after Ginzburg and Ben-Avraham, 1986, with modifications); (C) Quantitative interpretation of the Zema magnetic anomaly. The following parameters are taken from the anomaly plot (*characteristic point method*): d_1 = difference of semi-amplitude point abscissae, d_2 = difference of extremum abscissae, d_3 = difference of inflection point abscissae.

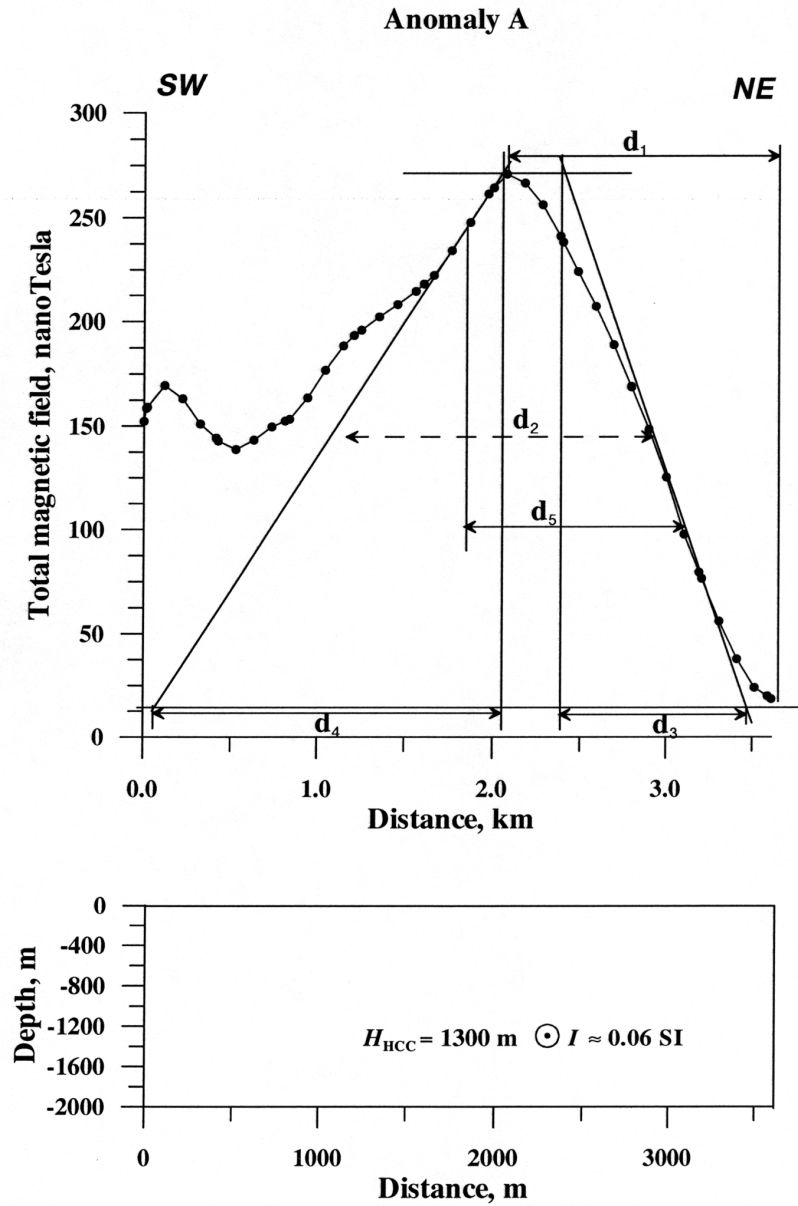


Fig. 6. Quantitative interpretation of anomaly A (see location in Fig. 2). Besides the *characteristic point method* (see caption to Fig. 5), here the *tangent method* was applied. The following terms are taken from the plot for the *tangent method*: d_3 = difference in abscissae of the points of intersection of an inclined tangent with horizontal tangents on one branch; d_4 = the same on the other branch (d_3 is selected from the plot branch with conjugated extremums).

meridional profile, i.e., the interpretation error was 2%). For the reverse anomaly C (HCC model) (Fig. 7) the obtained depth of the HCC center is 700 m. The upper edge of this body, by our calculations, is at the depth of 550 m. Two reverse magnetic anomalies—D and E—were interpreted using the TB model (Fig. 8). The depths of the upper edges of these disturbing

bodies were determined at 325 and 460 m, respectively. Other anomalies (F–L) were analyzed in the same manner.

The determined depths of the magnetic sources (upper edge) range from 1100–1200 m (anomalies A and L) to 300 m (anomaly J). The obtained target magnetization values range between 0.015 to 0.06 SI

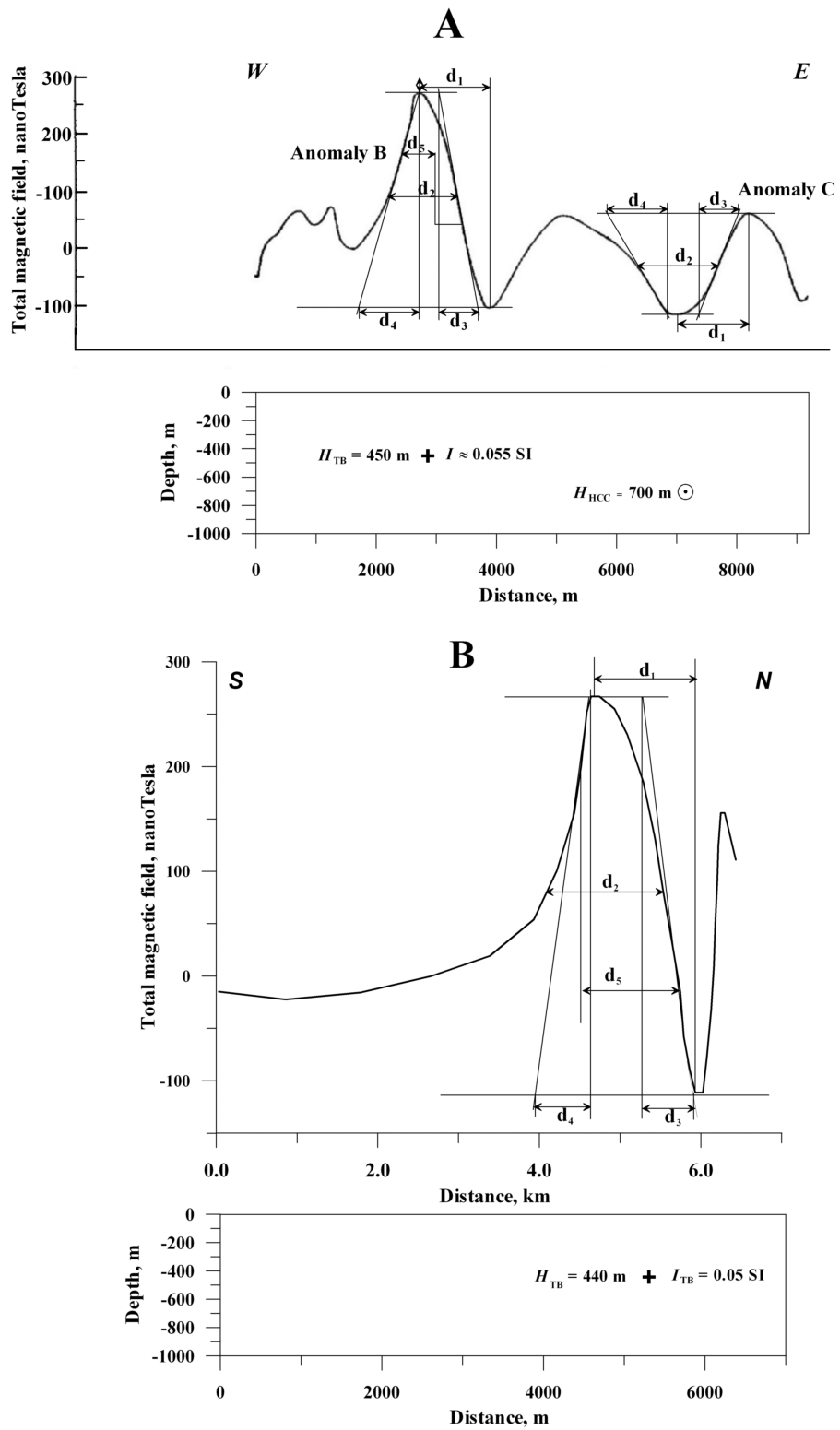


Fig. 7. A: Quantitative interpretation of anomalies B and C along latitudinal profile 252. B: Quantitative interpretation of anomaly B along meridional profile 204 (see location in Fig. 2).

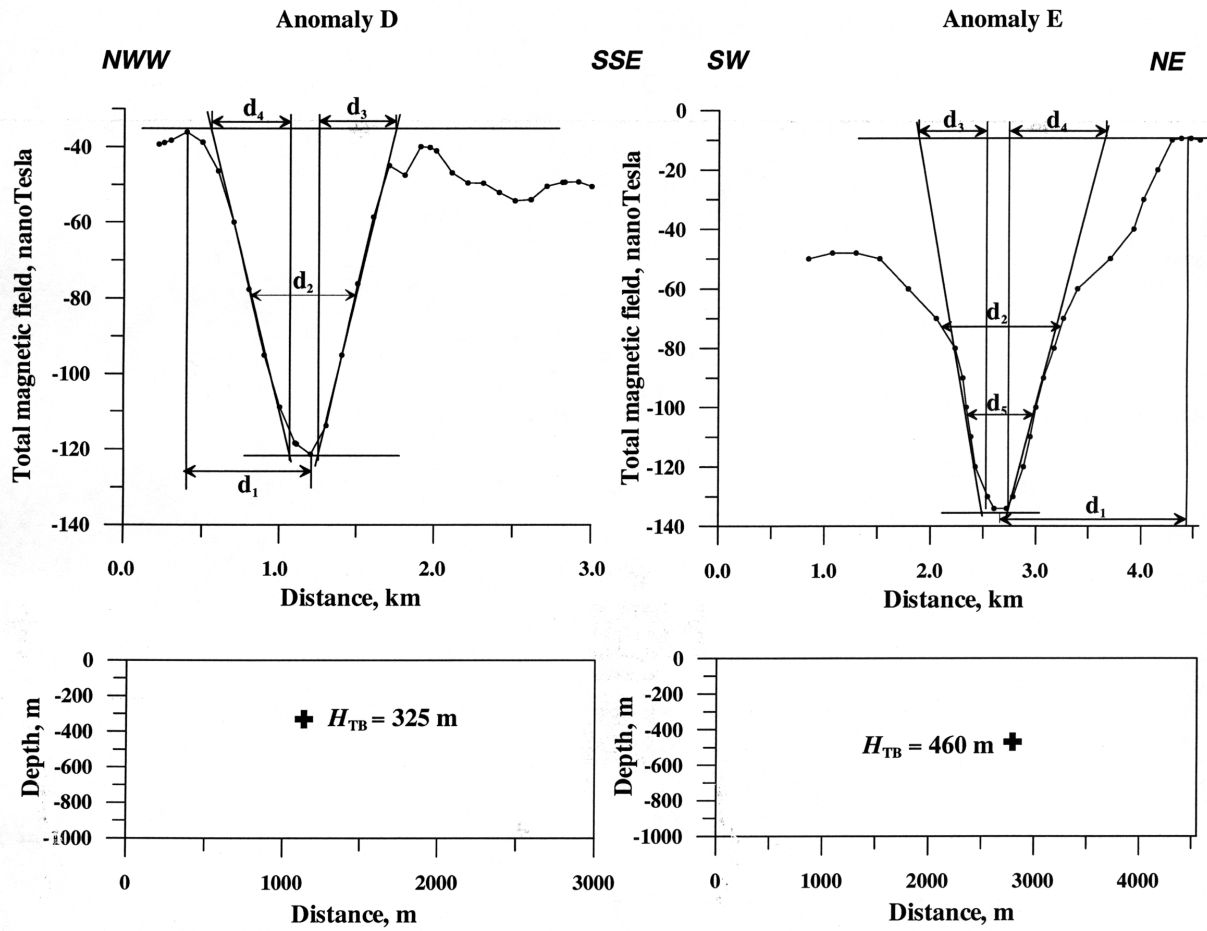


Fig. 8. Quantitative interpretation of anomalies D and E (see location in Fig. 2).

Table 1
Elevation of basaltic formation roof in areas surrounding Lake Kinneret

Structure	Small surface basaltic occurrences: Maximal and minimal points in meters			
	Western part	Eastern part	Northern part	Southern part
Korazim Plateau		+408	-125 – -200	
Ginosar Valley	-50	-175		
Lower Galilee	368	-150		
Kinarot Basin			-676*, -98**	-210
Golan Heights (SW part)	-175 – -190	300 – 375		

Sign “-” refers to elevation below sea level.

*Observations in Zemah 1 well (after Marcus and Slager, 1985).

**Tel Katzir Block.

3-D magnetic field modeling

Confirming the results of the quantitative interpretation

3-D modeling was applied for testing the interpretation results obtained at the previous stage. A GSFC program was used for the modeling. The basic algorithm in the GSFC program provides the solution for the direct 3-D problem of gravity and magnetic prospecting for a horizontal polygonal prism limited in the strike direction. The program is capable of simultaneous computation of the gravity and magnetic fields at different levels from the arbitrary complex geological media. The developed algorithm (Khesin et al., 1996) allowed us to calculate magnetic anomalies with different values of inclination and declination for host medium and anomalous object, various azimuths of

investigated profiles, and various geometrical forms of modeled objects. Figure 9 illustrates an example of 3-D modeling of the magnetic field over anomaly E—produced by a reversely magnetized object. The observed and calculated graphs are in good agreement (Fig. 9) (the right part of the observed curve is disturbed, apparently by the influence of neighboring anomalies). The results of the modeling are in line with the data obtained at the previous stage of the inverse problem solution.

3-D modeling of the reversely magnetized rocks along profile 210

As can be inferred from the review of paleomagnetic investigations in the areas surrounding Lake Kinneret (Freund et al., 1965; Nur and Helsey, 1971; Mor and Steinitz, 1982, 1985; Ron et al., 1984;

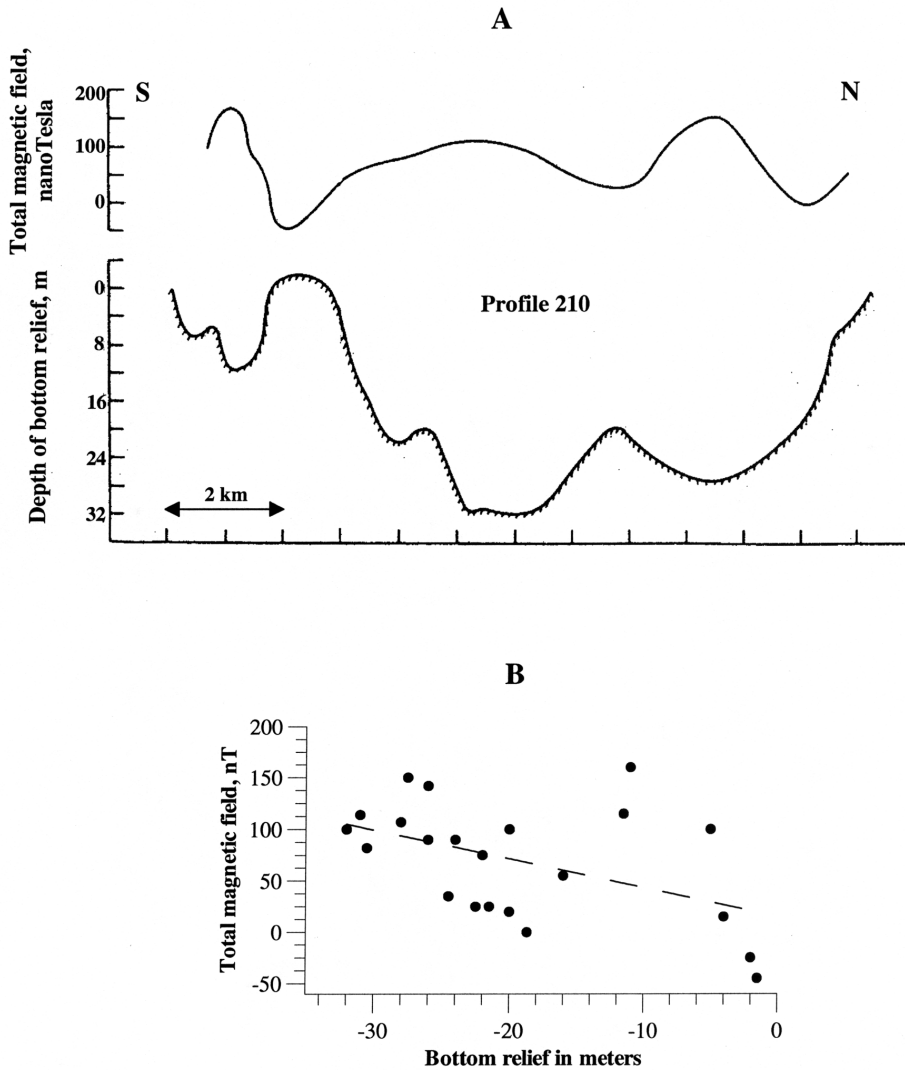


Fig. 10. (A) Comparison between the graphs of ΔT intensity and bottom relief, profile 210 (after Ben-Avraham et al., 1980). (B) correlation field between the two parameters (dashed line shows linear approximation).

Heimann, 1990; Shaliv, 1991; Heimann and Ron, 1993; Heimann et al., 1996), a variety of basaltic samples with a reverse magnetization was identified.

The complex structure of the eastern part of Lake Kinneret was noted by many researchers (for instance, Michelson et al., 1987; Ben-Avraham et al., 1996). Profile 210 (data from Ben-Avraham et al., 1980), located in the eastern part of lake (Fig. 2), indicates an interesting peculiarity of the section: an inverse correlation between the registered total magnetic anomaly field ΔT and the bottom relief (Fig. 10A). We suggest that the reversely magnetized rocks at or near the lake's bottom cause this effect. The least-square

method was applied for calculating the correlation coefficient r between the ΔT and the bottom relief (Fig. 10B). The comparatively modest coefficient value, -0.7 , may be explained by the influence of oblique magnetization, which distorts the magnetic effect from the projection of the bottom relief highs to the lake water level (level of magnetic observations). The 3-D modeling using the GSFC program allowed estimating the value of magnetization and the location of the magnetization vector in the space: 3,500 mA/m and -65° , respectively (Fig. 11). Based on the ages and polarities around the lake, we propose that these reversely magnetized basalts are of the Early Pliocene.

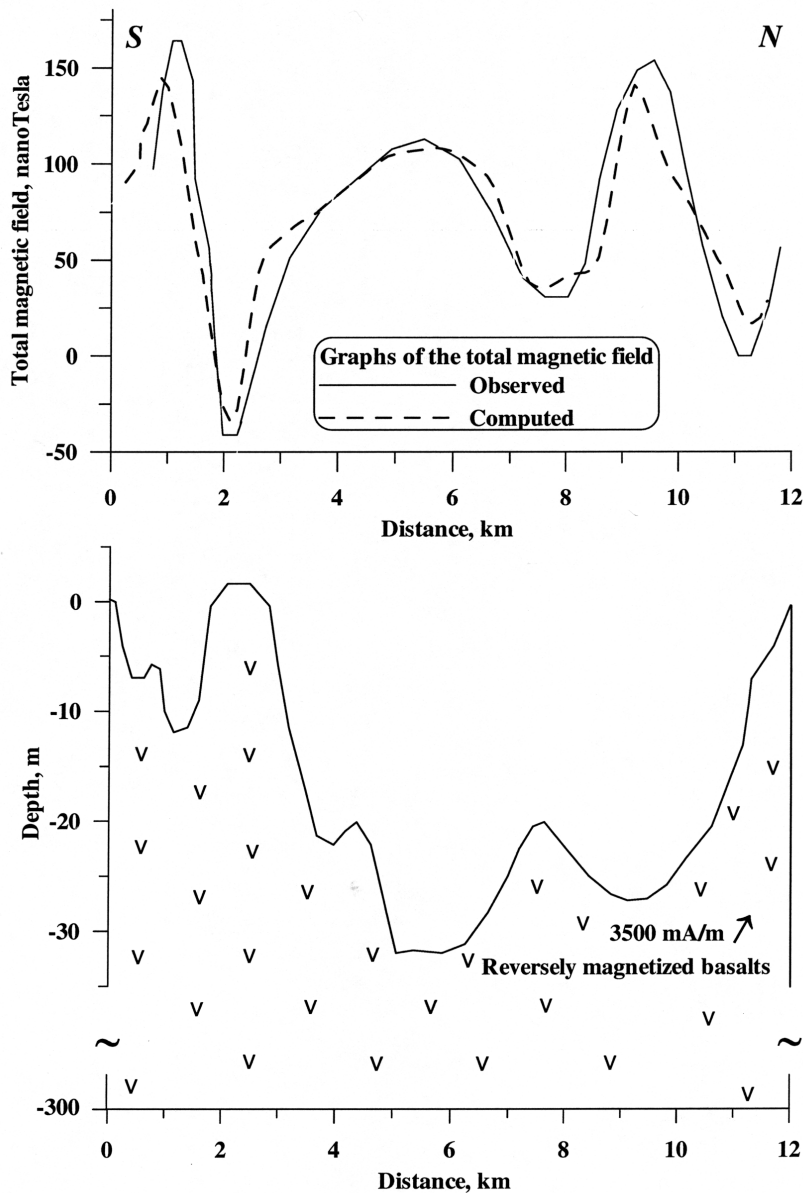


Fig. 11. 3-D modeling of the magnetic field over the reversely magnetized basalts (profile 210). Arrow indicates the direction of the magnetization vector.

Distribution of basalts in the Kinneret basin: 3-D estimation

The Cover Basalt in the Golan Heights is 550 m above Lake Kinneret (Heimann et al., 1996). The Cover Basalt in Zemah 1 well is about 500 m below Lake Kinneret (Marcus and Slager, 1985). The absence of significant magnetic anomalies in the central part of the lake is explained by post-basalt sedimentary basin fill (Eppelbaum and Ben-Avraham, 2000). 3-D modeling of the magnetic field allowed us to estimate an occurrence of separate magnetic sources at the depth of 1.1–1.3 km. Figure 12 illustrates an example of such magnetic field analysis along profile S–S (location of this profile is presented in Fig. 2). At the first stage an observed magnetic anomaly L (HCC approximation model was used) was quantitatively interpreted (Fig. 12A). The obtained data were utilized for the second stage, 3-D modeling of the magnetic field. Comparison of observed (averaged) and computed magnetic fields over the developed physical–geological model is shown in Fig. 12B. The upper surface of the identified magnetic body is at the depth of 1250 m; it has magnetization of 3000 mA/m with location of the magnetized vector of 30°. The generalized results of the quantitative interpretation of the magnetic anomalies and 3-D modeling of magnetic field are presented in Fig. 13.

BASALTS AROUND LAKE KINNERET: PALEOMAGNETIC AND RADIOMETRIC CHARACTERISTICS

Flood basalts are exposed in a series of fault-bounded blocks surrounding Lake Kinneret. More than 80% of the basalts surrounding Lake Kinneret belong to the Pliocene Cover Basalt flows, which is 150–200 m thick outside the rift valley, but reaches about 700 m in the Zemah 1 well, inside the valley (Marcus and Slager, 1985). The elevations of basaltic formations in the Lake Kinneret area are summarized in Table 1.

Paleomagnetic characteristics of basalt sequences

Classification of basaltic sequences may be effectively performed using methods of paleomagnetic stratigraphy (Butler, 1992). Several paleomagnetic investigations were carried out around Lake Kinneret. Paleomagnetic stratigraphy methods were used for studying the Late Pliocene–Pleistocene basalts in the northern part of the studied area, the Early Pliocene basalts at the Korazim Plateau (Heimann, 1990), and the Late Pleistocene basalts at Kinnarot Basin (Heimann and Braun, 2000).

In another study (Eppelbaum et al., 2004), the stratigraphic column of the studied area was compiled using the data from Heimann (1990), Braun et al. (1991), Shaliv (1991), Heimann and Ron (1993), the paleomagnetic reversals scale (Cande and Kent, 1992), and the international stratigraphic scale (Berggren et al., 1995).

Radiometric dating of the Pliocene and Quaternary basalts

The age of the Late Cenozoic basalts at the central Dead Sea Fault is based on over 300 radiometric dates (Heimann, 1990; Shaliv, 1991; Heimann et al., 1996). In the studied area, the radiometric age of the basalts was measured at more than 100 points (Middle Miocene–Pleistocene) (Eppelbaum et al., 2004, in press). From these data, 58 points (mainly belonging to Cover Basalts and partially of the uppermost Late Miocene, Late Pliocene, and Late Pleistocene) were selected.

INTEGRATED ANALYSIS OF SPATIAL LOCATION OF BASALTIC FORMATIONS

McDougall et al. (1977) have shown an effective integration of paleomagnetic analysis with radiometric dating for investigation of basaltic formations in western Iceland. Taking into account complexity of the geological structure of the Lake Kinneret area, we apply integrated magnetic/paleomagnetic radiometrically dated investigation with utilization of structural-tectonic characteristics of the area. We presented our interpretation in a magnetic–geological map of the Lake Kinneret area (Eppelbaum et al., 2004, in press) developed on the basis of the Geological Map of Israel (Sneh et al., 1998a). Radiometric data were generalized after Heimann (1990), Shaliv (1991), and Heimann et al. (1996), and paleomagnetic data after Freund et al. (1965), Nur and Helsey (1971), Mor and Steinitz (1982,1985), Ron et al. (1984), Heimann (1990), Shaliv (1991), Heimann and Ron (1993), and Heimann et al. (1996).

The map includes the main fault zones and sub-zones of the paleomagnetic polarities of the cover basalts, as well as the results of magnetic anomaly interpretation in the lake. The identification of selected paleomagnetic zones was done by way of correlation between the paleomagnetic and radiometric data in each tectonic block. The basalts span a nearly continuous sequence from the Late Pleistocene to the uppermost Late Miocene, recording polarity stages 1n, 2n, 2r, 2An, 2Ar, 3n, 3r, 3An, and 3Ar.

Most of the zones of normal and reverse polarity

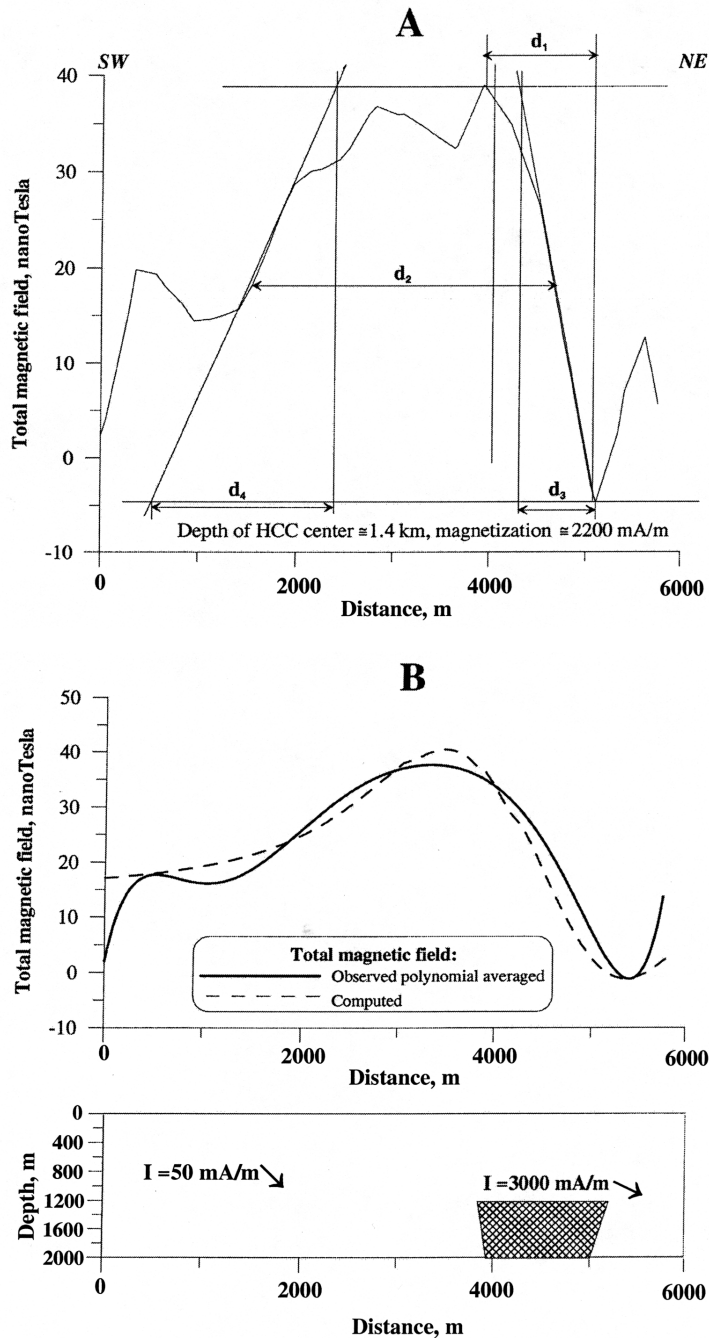


Fig. 12. Estimation of depth of magnetic anomalies in the central part of Lake Kinneret. (A) Observed anomaly along profile I-I with elements of interpretation. (B) 3-D modeling of magnetic field along profile S-S. Arrows in B show direction of the magnetization vector. Location of profile S-S is shown in Fig. 2 by a dashed line.

recognized in the western side of the lake (Fig. 15) can be correlated to adjacent zones in the lake's margins. However, the magnetic patterns on the eastern and northern parts of the lake cannot be directly continued onshore. This can be explained by shear and large displace-

ments on the east in contrast to downfaulting on the west. The presence of a narrow zone of reverse magnetization in the eastern part of Lake Kinneret (Fig. 10) is of particular interest. Two explanations are possible: (1) that this zone corresponds to paleomagnetic zone

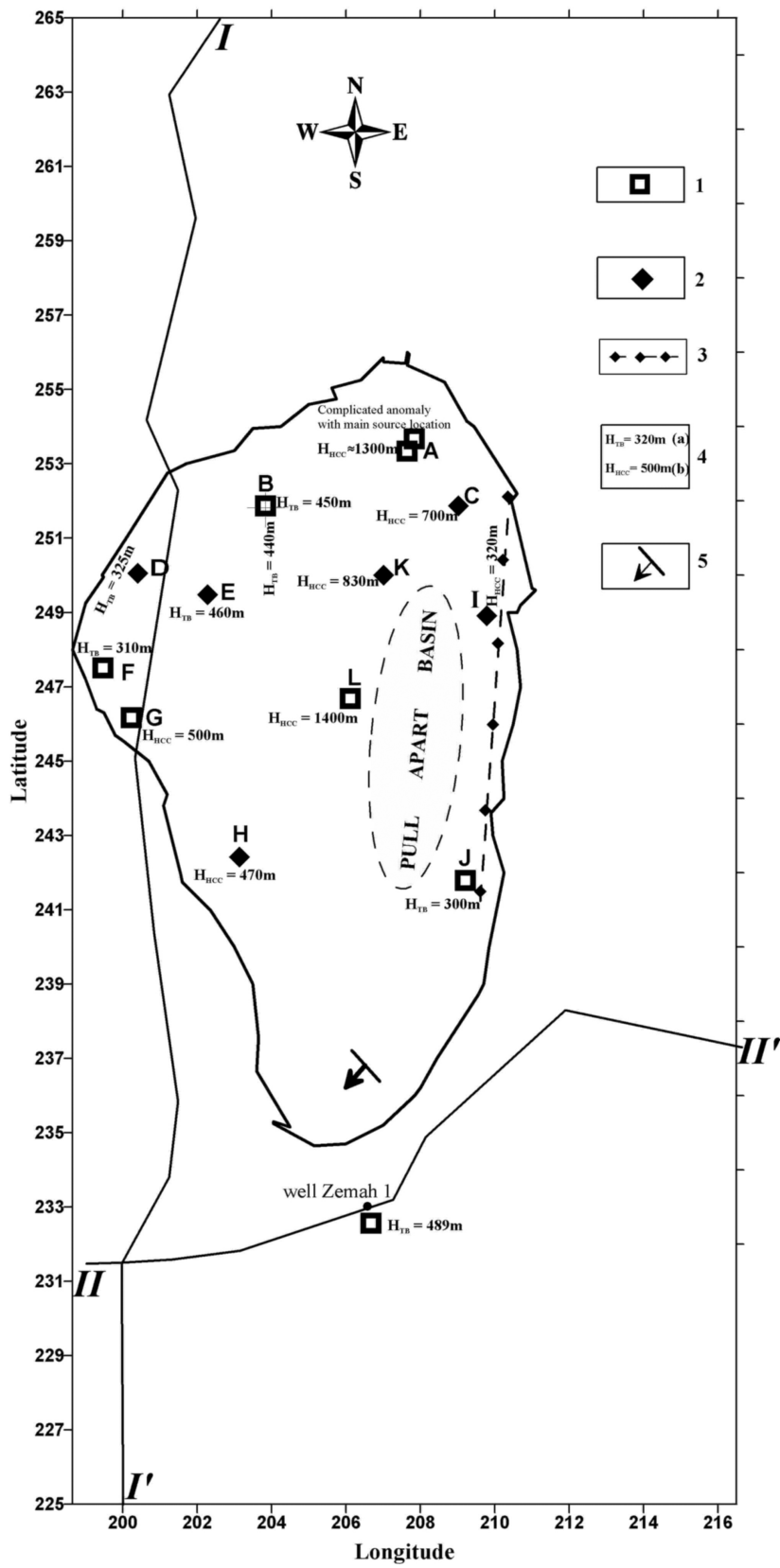


Fig. 13 facing page. Quantitative scheme of basalt distribution in Lake Kinneret. 1—location of magnetic anomaly with normal magnetization, 2—location of magnetic anomaly with reverse magnetization, 3—observed profile indicating reverse correlation between the total magnetic field and the relief of lake bottom, 4—calculated depth of the magnetic bodies occurring (lake level at -210 m m.s.l. was assumed as a zero surface): (a) H_{TB} —for the upper edge of thin bed, (b) H_{HCC} for the center of horizontal circular cylinder, 5—generalized direction of the proposed buried basaltic plate dipping. Pull-apart basin is contoured according to gravity (Ben-Avraham et al., 1996) and seismic (Ben-Gai and Reznikov, 1997) data. Lines I–I' and II–II' show the location of paleomagnetic profiles.

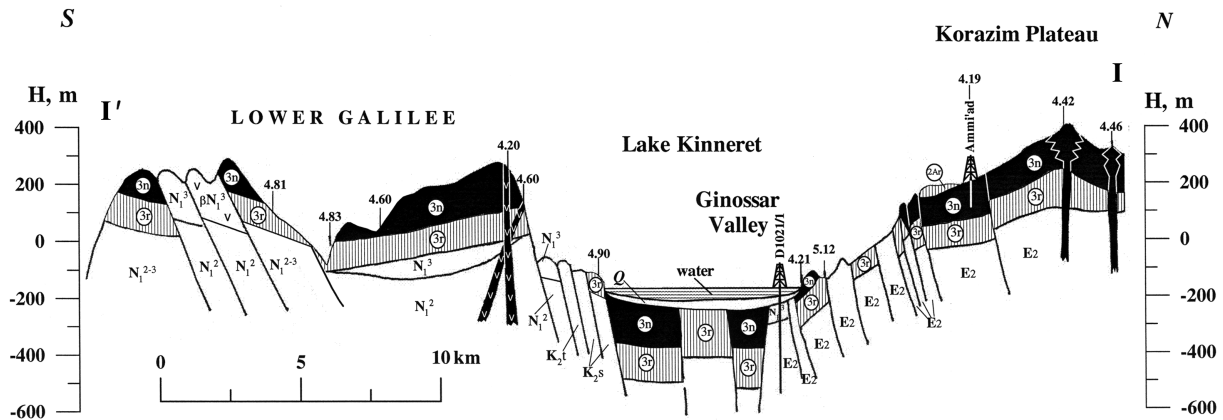


Fig. 14. Paleomagnetic profile along the line I–I' (see location in Fig. 13). 3n, 3r, and 2Ar are the indexes of paleomagnetic zones. At the Korazim Plateau and Lower Galilee paleomagnetic zones, 3r and 3n are dominant. The thicknesses of these zones within the rises and in the flanks of Lake Kinneret depression have similar values. Analysis of the magnetic anomalies in the western part of Lake Kinneret (Fig. 13) indicates that they are part of zones 3r and 3n.

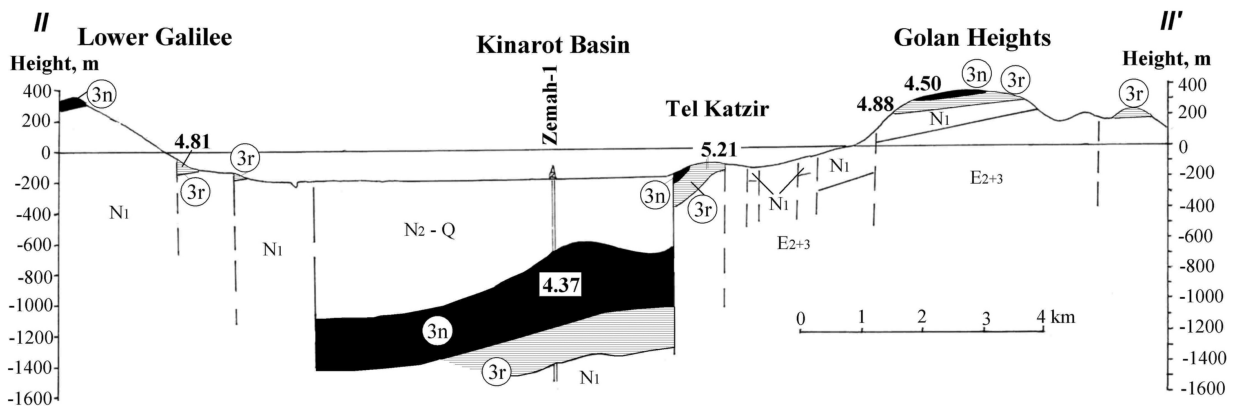


Fig. 15. Paleomagnetic profile along the line II–II' (see location in Fig. 13). Symbols are the same as in Fig. 14. This profile indicates dipping of thick zone 3n (Cover Basalt) from NE to SW.

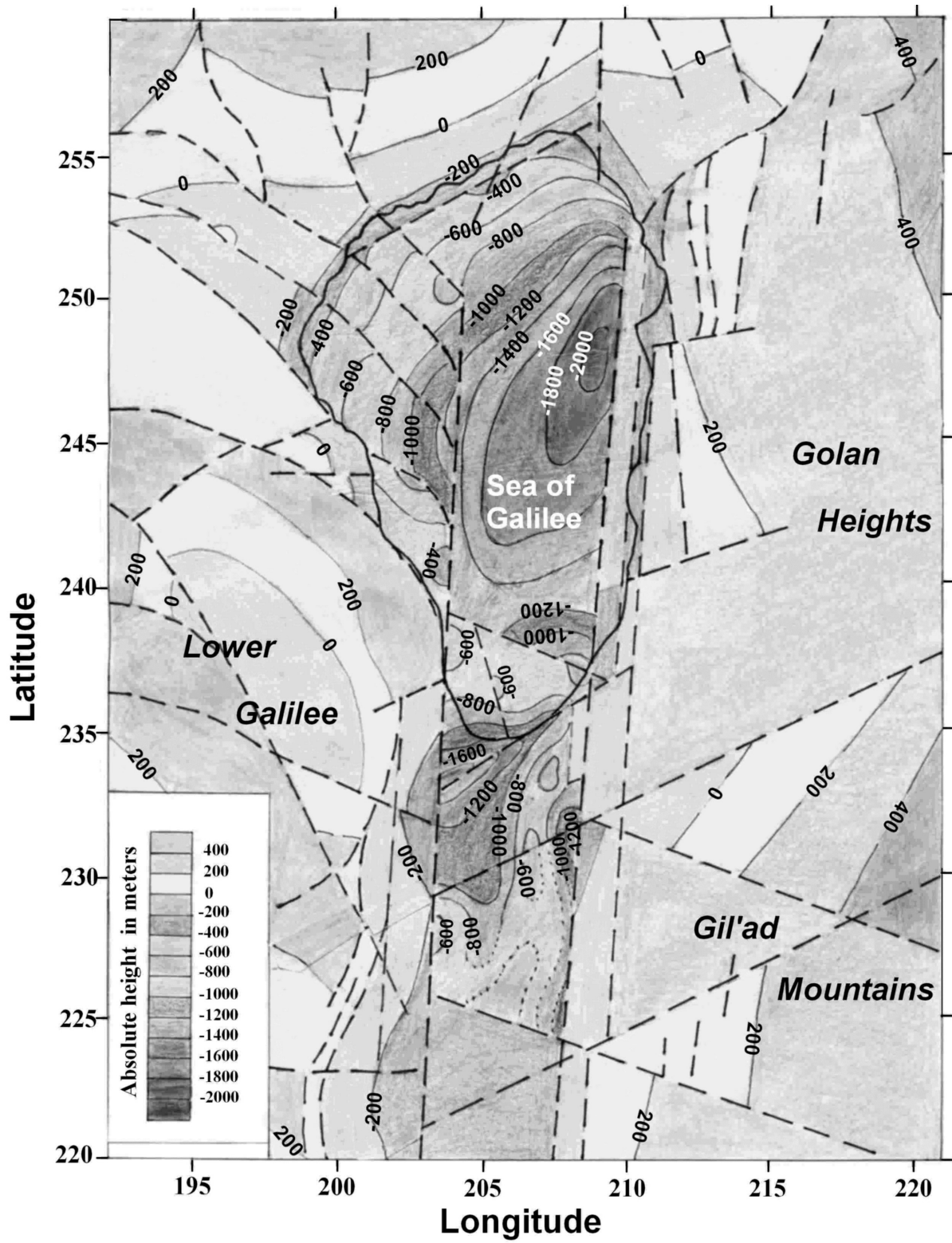


Fig. 16. Structural map of Cover Basalt surface in the Sea of Galilee and its vicinity (isolines are given in meters relative to mean sea level). Dashed lines designate location of faults.

3r, a submersed step of Cover Basalts, and (2) that this zone corresponds to intrusive associations of the younger paleomagnetic zone 2Ar.

A N–S paleomagnetic profile along the western part of the lake (Fig. 14, line I–I') shows that there are two topographic rises—in the south (Lower Galilee) and in the north (Korazim Plateau)—and a depression in the center of the profile, which corresponds to the shallow water part of Lake Kinneret. At the Korazim Plateau and Lower Galilee, paleomagnetic zones 3r and 3n are dominant. The thicknesses of these zones within the rises and in the flanks of the Lake Kinneret depression have similar values. Analysis of the magnetic anomalies in the western part of Lake Kinneret (Fig. 13) shows that they are part of zones 3r and 3n. Such a pattern indicates that the western part of the Lake Kinneret depression is probably a part of an inversion trough formed along the Pliocene uplift in the eastern part of Galilee (Matmon et al., 1999).

A SW–NE paleomagnetic profile along the Kinarot basin (Fig. 15, line II–II') supports results of 3-D modeling, indicating dipping of magnetized basaltic plate in the southern part of the lake from NE to SW at 9–12°. The results of magnetic and paleomagnetic data analysis with utilization of seismic (Ben-Avraham et al., 1981; Rotstein and Bartov, 1989; Rotstein et al., 1992; Ben-Gai and Reznikov, 1997; Hurwitz et al., 2002; Zurieli, 2002) and tectonic (Mor, 1986; Michelson et al., 1987; Ben-Avraham et al., 1990, 1996; Heimann, 1990; Shaliv, 1991; Heimann et al., 1996; Sneh et al., 1998b; Matmon et al., 1999; Belitzky, 2002) data were applied for the compilation of a structural map of Cover Basalt for Lake Kinneret and its vicinity (Fig. 16). Outside the lake, this map has been developed on the basis of the Geological Map of Israel (Sneh et al., 1998a).

CONCLUSIONS

For the analysis of magnetic sources (A–L) occurring in the lake, advanced methodology specially developed for complicated environments was applied. The determined depths of the magnetic sources (upper edge) range from 1100–1200 m (anomalies A and L) to 300 m (anomaly J). The obtained target magnetization values range between 0.015 and 0.06 SI units. The magnetic field pattern in the southern part of Lake Kinneret significantly differs from the magnetic field in other parts of the lake. The analysis of the magnetic field distribution, supported by structural-physical analysis, indicates that this pattern in the southern part of the lake is caused probably by a

magnetized basaltic plate dipping from NE to SW at 9–12°. Inverse correlation between the magnetic field and bottom relief in the eastern part of the lake indicates possibly at or near-surface basalt occurrence of the Early Pliocene. The anomalous zones on the western and northern parts of the lake are in accordance with the adjacent paleomagnetic zones on shore. The anomalies on the eastern and southern parts do not show the same agreement. We suggest that the eastern part is sheared and displaced by the sinistral movement on the main boundary fault. We further suggest that the central part of the lake is a pull-apart basin, and the western part is a subsided continuation of the Eastern Galilee. The depth of Cover Basalt under the lake as determined from magnetic analysis is in agreement with the depth derived from the seismic reflection profiles.

ACKNOWLEDGMENTS

Partial support for this study was provided by the Ministry of Infrastructure and Energy of Israel, grant ES-31-99. We thank Dr. Rami Weinberger (Geological Survey of Israel, Jerusalem), Prof. D.S. Parasnis (Luleå University, Sweden), and one anonymous reviewer for their valuable comments. We are grateful to Dr. Margaret Reznikov (The Geophysical Institute of Israel, Lod) for useful discussion.

REFERENCES

- Bartov, Y. 1979. Israel-Geological Map 1:500,000. Geological Survey of Israel, Jerusalem, Israel.
- Belitzky, S. 2002. The structure and morphotectonics of the Gesher Benot Ya'aqov area, northern Dead Sea Rift, Israel. *Quat. Res.* 58: 372-380.
- Ben-Avraham, Z., Hänel, R., Villinger, H. 1978. Heat flow through the Dead Sea rift. *Mar. Geol.* 28: 253-269.
- Ben-Avraham, Z., Shosham, Y., Klein, E., Michelson, H., Serruya, C. 1980. Magnetic survey of Lake Kinneret—central Jordan Valley, Israel. *Mar. Geophys. Res.* 4: 257-276.
- Ben-Avraham, Z., Ginzburg, A., Yuval, Z. 1981. Seismic reflection and refraction investigation of Lake Kinneret—Central Jordan Valley, Israel. *Tectonophysics* 80: 165-181.
- Ben-Avraham, Z., Shaliv, G., Nur, A. 1986. Acoustic reflectivity and shallow sedimentary structure in the Sea of Galilee—Jordan Valley. *Mar. Geol.* 70: 175-189.
- Ben-Avraham, Z., Amit, G., Golan, A., Begin, Z.B. 1990. The bathymetry of Lake Kinneret and its structural significance. *Isr. J. Earth Sci.* 39: 77-84.
- Ben-Avraham, Z., ten-Brink, U., Bell, R., Reznikov, M. 1996. Gravity field over the Sea of Galilee: evidence for a

- composite basin along a transform fault. *J. Geophys. Res.* 101: 533–544.
- Ben-Gai, Y., Reznikov, M. 1997. Seismic multi-channel survey in Lake Kinneret. Report No. 733/167/97, The Geophysical Institute of Israel.
- Berggren, W.A., Hilgen, F.J., Langereis, C.G., Kent, D.V., Obradovich, J.D., Raffi, I., Raymo, M.E., Shackleton, N.J. 1995. Late Neogene chronology: new perspectives in high resolution stratigraphy. *Geol. Soc. Am. Bull.* 107(11): 1272–1287.
- Blakely, R.J. 1995. Potential theory in gravity and magnetic applications. Cambridge Univ. Press, Cambridge, 435 pp.
- Braun, D., Ron, H., Marco, S. 1991. Magnetostratigraphy of the hominid tool-bearing Erk el Ahmar Formation in the northern Dead Sea Rift. *Isr. J. Earth Sci.* 40: 191–197.
- Butler, R.F. 1992. Paleomagnetism: magnetic domains of geological terranes. Blackwell Scientific Publ., Oxford, 319 pp.
- Cande, S., Kent, D.V. 1992. A new geomagnetic polarity time scale for the Late Cretaceous and Cenozoic. *J. Geophys. Res.* 97, (B10): 13,917–13,951.
- Cornee, J.J., Roger, S., Munch, P., Saint Martin, J.P., Feraud, G., Conesa, G., Pestrea-Sain Martin, S. 2002. Messinian events: new constrains from sedimentological investigations and new $^{40}\text{Ar}/^{39}\text{Ar}$ ages in the Melilla-Nador Basin (Morocco). *Sediment. Geol.* 151: 127–147.
- Eppelbaum, L.V., Ben-Avraham, Z. 2000. Sea of Galilee (Israel): comprehensive analysis of magnetic anomalies. *Trans. of the 1st S. Mueller Conf. of the EGS, Dead Sea, Israel*, p. 31 (Abstract).
- Eppelbaum, L., Khesin, B., Ginzburg, A., Ben-Avraham, Z. 1992. Quantitative interpretation of magnetic anomalies and preliminary 3-D modeling of gravity and magnetic fields. *Annu. Mtg. Isr. Geol. Soc., Ashqelon*, p. 35 (Abstract).
- Eppelbaum, L., Ben-Avraham, Z., Katz, Y. 2004. Integrated analysis of magnetic, paleomagnetic and K-Ar data in a tectonic complex region: an example from the Sea of Galilee. *Geophys. Res. Lett.*, in press.
- Flexer, A., Yellin-Dror, A., Kronfeld, J., Rozenthal, E., Ben-Avraham, Z., Artsztein, P., Davidson, L. 2000. A Neogene salt body as the primary source of salinity in Lake Kinneret. *Arch. Hydrobiol. Spec. Iss. Advanc. Limnol.* 55: 69–85.
- Folkman, Y., Yuval, Z. 1976. Aeromagnetic Map of Israel, 1:250,000. Israel Institute for Petroleum Research and Geophysics, Holon, Israel.
- Freund, R. 1970. The geometry of faulting in Galilee. *Isr. J. Earth Sci.* 19: 117–140.
- Freund, R., Oppenheim, M.J., Schulman, N. 1965. Direction of magnetization of some basalts in the Jordan Valley and Lower Galilee (Israel). *Isr. J. Earth Sci.* 14: 37–74.
- Freund, R., Garfunkel, Z., Zak, I., Goldberg, M., Wessbrod, T., Derin, B. 1970. The shear along the Dead Sea Rift. *Philos. Trans. R. Soc. London, Ser. A* 267: 107–130.
- Garfunkel, Z. 1989. Tectonic setting of Phanerozoic magmatism in Israel. *Isr. J. Earth Sci.* 38: 51–74.
- Garfunkel, Z., Zak, I., Freund, R. 1981. Active faulting in the Dead Sea Rift. *Tectonophysics* 80: 1–26.
- Ginzburg, A., Ben-Avraham, Z. 1986. Structure of the Sea of Galilee Graben, Israel, from magnetic measurements. *Tectonophysics* 126: 153–164.
- Golani, U. 1962. The geology of Lake Tiberias region and the hydrogeology of the saline springs. Water Planning for Israel Ltd. (TAHAL), Geotech Dept., Rep. No. 19.
- Goldman, M., Hurwitz, S., Gvirtzman, H., Rabinovich, B., Rotstein, Y. 1996. Application of the marine time-domain electromagnetic method in lakes: the Sea of Galilee, Israel. *Eur. J. Environ. Eng. Geophys.* 1: 125–138.
- Hazan, N., Agnon, A., Stein, M., Nadel, D., Marco, S. 2002. The history of Lake Kinneret in the last 40,000 years: sedimentological and archaeological evidence. In: *Guide to Excursion. Annu. Mtg. Isr. Geol. Soc., Ma'agan*, pp. 39–55 (in Hebrew).
- Heimann, A. 1990. The development of the Dead Sea Rift and its margins in northern Israel during the Pliocene and Pleistocene. Ph.D. thesis, Hebrew Univ., Jerusalem, 114 pp. (in Hebrew, English summary).
- Heimann, A., Braun, D. 2000. Quaternary stratigraphy of the Kinnarot Basin, Dead Sea Transform, northeastern Israel. *Isr. J. Earth Sci.* 49: 31–44.
- Heimann, A., Ron, H. 1993. Geometric changes of plate boundaries along part of the northern Dead Sea transform: Geochronologic and paleomagnetic evidence. *Tectonics* 12: 477–491.
- Heimann, A., Steinitz, G. 1989. $^{40}\text{Ar}/^{39}\text{Ar}$ total gas age of basalts from the western slopes of the Golan Heights. *Geol. Surv. Isr., Current Res.* 6: 29–32.
- Heimann, A., Steinitz, G., Mor, D., Shaliv, G. 1996. The Cover Basalt Formation, its age and its regional and tectonic setting: implications from K-Ar and $^{40}\text{Ar}/^{39}\text{Ar}$ geochronology. *Isr. J. Earth Sci.* 45: 55–71.
- Hurwitz, S., Garfunkel, Z., Ben-Gai, Y., Reznikov, M., Rotstein, Y., Gvirtzman, H. 2002. The tectonic framework of a complex pull-apart basin: seismic reflection observations in the Sea of Galilee, Dead Sea transform. *Tectonophysics* 359: 289–306.
- Iliani, S., Harlavan, Y., Tarawhen, K., Rabba, I., Weinberger, R., Ibrahim, K., Peltz, S., Steinitz, G. 2001. New K-Ar ages of basalts from Harrat Ash-Shaam volcanic field in Jordan: implications for the span and duration of the upper-mantle upwelling beneath the western Arabian Plate. *Geology* 29: 171–174.
- Katz, Y.I., Eppelbaum, L.V. 1999. Preliminary results of basin mapping of the Lower Cretaceous traps in northern Israel. *Annu. Mtg. Isr. Geol. Soc., Dead Sea, Israel*, p. 40 (Abstract).
- Khesin, B.E., Alexeyev, V.V., Eppelbaum, L.V. 1996. Interpretation of geophysical fields in complicated environments. *Modern approaches in geophysics*. Kluwer Academic Publishers, Dordrecht, 367 pp.
- Krijgsman, W., Hilgen, F.G., Langereis, C.G., Santarelli, A., Zachariasse, W.J. 1995. Late Miocene magnetostrati-

- graphy, biostratigraphy and cyclostratigraphy in the Mediterranean. *Earth Planet. Sci. Lett.* 136: 475–494.
- Marcus, E., Slager, J. 1985. The sedimentary-magmatic sequence of the Zemah 1 well (Jordan–Dead Sea Rift, Israel) and its emplacement in time and space. *Isr. J. Earth. Sci.* 34: 1–10.
- Marco, S., Agnon, A., Ellenblum, R., Eidelman, A., Basson, U., Boas, A. 1997. 817 year old walls offset sinistrally 2.1 m by the Dead Sea Transform, Israel. *J. Geodynamics* 24 (1–4): 11–20.
- Marco, S., Hartal, M., Hazan, N., Lev, L., Stein, M. 2003. Archaeology, history, and geology of the A.D. 749 earthquake, Dead Sea transform. *Geology* 31(8): 665–668.
- Matmon, A., Enzel, Y., Zilberman, E., Heimann, A. 1999. Late Pliocene and Pleistocene reversal of drainage systems in northern Israel: tectonic implications. *Geomorphology* 28: 43–59.
- Matmon, A., Wdowinski, S., Hall, J.K. 2003. Morphological and structural relations in the Galilee extensional domain, northern Israel. *Tectonophysics* 371: 223–241.
- McDougall, I., Saemundsson, K., Johannesson, H., Watkins, N.D., Kristjansson, L. 1977. Extension of the geomagnetic polarity time scale to 6.5 m.y.: K-Ar dating, geological and paleomagnetic study of a 3,500-m lava succession in western Iceland. *Geol. Soc. Am. Bull.* 88: 1–15.
- Michelson, H. 1972. The hydrogeology of southern Golan Heights. Water Planning for Israel Ltd. (TAHAL), Rep. HR/72/037, 89 pp. (in Hebrew).
- Michelson, H., Flexer, A., Erez, Z. 1987. A comparison of the eastern and western sides of the Sea of Galilee and its implication on the tectonics of the northern Jordan Rift Valley. *Tectonophysics* 141: 125–134.
- Mor, D. 1986. The volcanism of the Golan Heights. Ph.D. thesis, Hebrew Univ., Jerusalem, 170 pp. (in Hebrew, English summary).
- Mor, D., Steinitz, G. 1982. K-Ar age of the cover basalts surrounding the Sea of Galilee. *Geol. Survey Isr., Rep. Me/6/82*, 14 pp.
- Mor, D., Steinitz, G. 1985. K-Ar ages of the Neogene-Quaternary basalts around the Yarmuk Valley. *Annu. Mtg. Isr. Geol. Soc.:* 77–78 (Abstract).
- Neev, D. 1978. The geology of Lake Kinneret. Kinneret – Assemblage of Scientific Articles. Publ. Lake Kinneret Auto., Zemah, Israel (in Hebrew).
- Nur, A., Helsey, C.F. 1971. Palaeomagnetism of Tertiary and Recent lavas of Israel. *Earth Planet. Sci. Lett.* 10: 375–379.
- Parasnis, D.S. 1997. Principles of Applied Geophysics. 5th ed., Chapman and Hall, London, 429 pp.
- Rao, D.A., Babu, H.V. 1984. On the half-slope and straight-slope methods of basement depth determination. *Geophysics* 49(8): 1365–1368.
- Roest, W.R., Verhoef, J., Pilkington, M. 1992. Magnetic interpretation using the 3-D analytic signal. *Geophysics* 57, No. 1: 116–125.
- Ron, H., Freund, R., Garfunkel, Z., Nur, A. 1984. Block rotation by strike-slip faulting: structural and paleomagnetic evidence. *J. Geophys. Res.* 89P: 6256–6270.
- Rotstein, Y., Bartov, Y. 1989. Seismic reflection across a continental transform: an example from a convergent segment of the Dead Sea rift. *J. Geophys. Res.* 94: 2902–2912.
- Rotstein, Y., Bartov, Y., Freislander, U. 1992. Evidence for local shifting of the main fault and changes in the structural setting, Kinarot basin, Dead Sea transform. *Geology* 20: 251–254.
- Saltsman, U. 1964. The geology of Tabha-Hukok-Migdal area. Water Planning for Israel (TAHAL), Rep. P. M. 374.
- Shaliv, G. 1991. Stages in the tectonics and volcanic history of the Neogene basin in the Lower Galilee and the valleys. Ph.D. thesis, Hebrew Univ., Jerusalem, 94 pp. (in Hebrew, English summary).
- Sneh, A., Bartov, Y., Rozenshaft, M. 1998a. Geological Map of Israel, Scale 1:200,000. Geological Survey of Israel, Ministry of National Infrastructure, Jerusalem.
- Sneh, A., Lang, B., Halicz, L. 1998b. The Sheikh Ali Fault, The Lake Kinneret, implications of new volcano-stratigraphic findings. *Geol. Survey of Israel, Current Res.* 11: 42–44.
- Schulman, N. 1966. The cross-faulted structure of Tiberias. *Israel. Isr. J. Earth Sci.* 15: 165–169.
- Telford, W.M., Geldart, L.D., Sheriff, R.E. 1999. Applied geophysics. Cambridge Univ. Press, Cambridge, 805 pp.
- Thurston, J.B., Smith, R.S. 1997. Automatic conversion of magnetic data to depth, dip, and susceptibility contrast using the SPI^m method. *Geophysics* 62, (3): 807–813.
- Weinstein, Y., Navon, O., Lang, B. 1994. Fractionation of Pleistocene alkali-basalts from the northern Golan Heights, Israel. *Isr. J. Earth Sci.* 43: 63–79.
- Zurieli, A. 2002. Structure and neotectonics in Kinarot Valley based on high-resolution seismic reflection. M.Sc. thesis, Tel Aviv University, 92 pp. (in Hebrew, English summary).